FINAL REPORT

ELECTROCHEMICAL APPROACH FOR PASSIVATING STEEL AND OTHER METALS AND FOR THE SIMULTANEOUS PRODUCTION OF A BIOCIDE TO RENDER WATER POTABLE

Contract No. NAS 9-12042

July 30, 1972

Prepared for:

National Aeronautics and Space Administration
Manned Spacecraft Center
Houston, Texas 77058

INSTITUTE FOR RESEARCH, INC.
1714 Rice Blvd.
Houston, Texas   77005

INSTITUTE FOR RESEARCH, INC.

1714 RICE BOULEVARD • HOUSTON, TEXAS 77005 • JA 6-4093

SUMMARY

Potentiostatic polarization curves indicated that
the cathodic reactions in deaerated $KI-I_2$ water solutions were
due to iodine reduction and hydrogen evolution. In the pres-
ence of oxygen an additional reduction wave appeared.

Anodic polarization curves revealed that iodine
could be produced in the region of potential from +600 to
+1000 mv vs. SCE.

The Beckman iodine meter was used to measure iodine
production rates. At an iodide concentration of 382 ppm,
maximum rates of 0.62 ± 0.03 ppm of iodine/min were measured
from +800 to +900 mv. These rates were measured in a two com-
partment cell which had been found to be better suited for
iodine production. The iodine production was dependent on
the rate of stirring (convection), and it was observed that
at relatively slow rates (~50 rpm) the production of iodine
was the greatest and diminished rapidly at rates greater than
75 rpm and potentials were unstable. Since all of the solutions
were dilute (approximately 382 ppm I^-), the solution resistance
was high. Faster stirring may have induced strong currents and
potentials or the potentiostat may not have been able to quickly
adapt to changes in these solutions. At potentials more anodic
than +900 mv, iodine may have been further oxidized to iodate.
However, at slow stirring rates and in a two compartment cell,
iodine was clearly produced.

-1-

I.

INTRODUCTION

Before iodine production rates were measured,
potentiostatic polarization curves were investigated in order
to determine the potential range through which electrochemical
reactions of interest occurred on 321 stainless steel in the
$KI-I_2$ water system. From these data the potential range from
+600 to +1000 mv vs. SCE was selected as the range of most
interest for iodine production.

Iodine production rates were then measured as a
function of potential. Effects of cell design and stirring
upon these rates were also investigated.

II.

POLARIZATION CURVES

The first experiments performed were to measure
cathodic and anodic polarization curves in solutions contain-
ing 1000 ppm of KI and 500 ppm of I_2. The potentiostatic
polarization circuit used was a typical three electrode cir-
cuit as shown in Figure 1. Constant potentials were maintained
by a Wenking potentiostat and measured on a Keithley 610C
Electrometer. Currents were measured on a Sensitive Research
microammeter. Solution resistances were measured by applying
a constant current from a pulse generator and then recording
the potential-time characteristics on a Tektronix Type 531A
Oscilloscope, with a Type D plug-in unit. This circuit is
shown in Figure 2.

At first the solutions were bubbled for at least
eight (8) hours with helium which had passed over charcoal
at liquid nitrogen temperatures. This was done in order to
eliminate complications due to oxygen in the $KI-I_2$ solutions.
However, a check of the iodine concentration by soluble starch
indicator revealed that this purification procedure lowered the
iodine concentration below the level that could be detected
by this indicator. A typical polarization curve in these
deaerated solutions is shown by curve A in Figure 3. From
open circuit of +445 mv vs. SCE (saturated calomel electrode)
to about -700 mv, cathodic currents were small (about 2 µamp/
cm^2. From -700 mv to more negative values, the current in-
creased due to hydrogen evolution. Anodic currents increased
in an irregular fashion and were much larger than cathodic
currents. This indicated that the general cathodic reaction

FIGURE 1
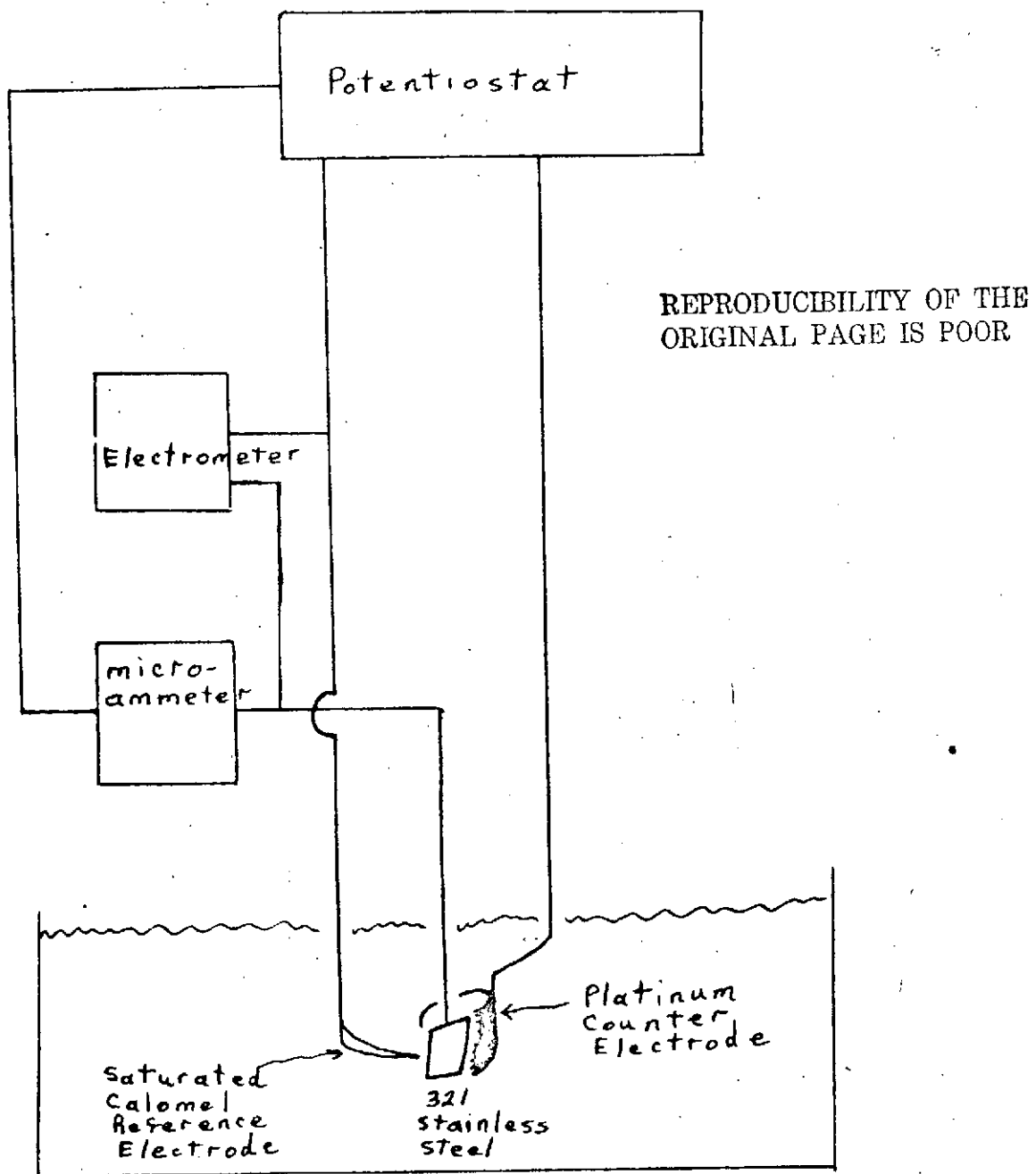
Schematic Diagram of the Circuit Used
to Maintain a Constant Potential

FIGURE 2
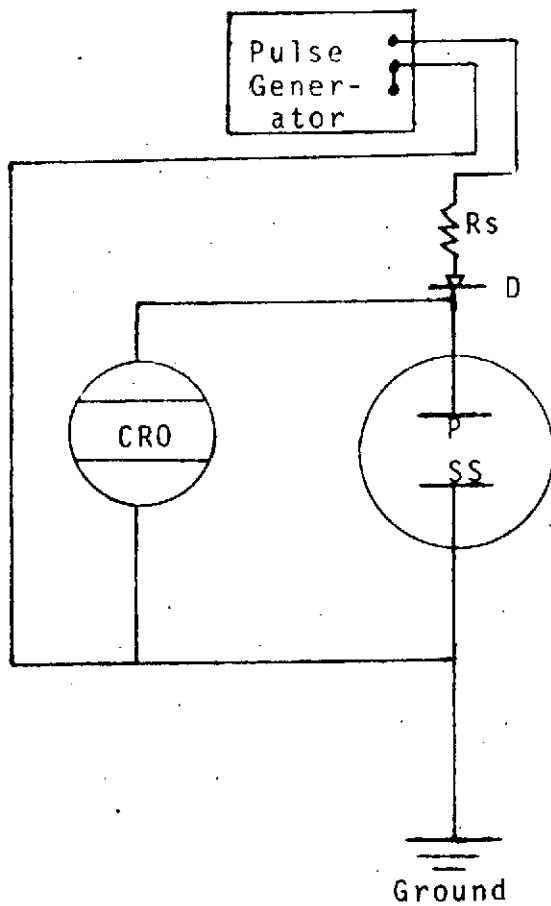
Rs = standard resistor
D = diode
CRO = oscilloscope
P = platinum counter
electrode
SS = 321 stainless steel
electrode

Electrical Circuit for Solution
Resistance Measurements

Helium had been bubbling for several hours; the concentration of oxygen was very small.

No helium

A

B

REPRODUCIBILITY OF THE ORIGINAL PAGE IS POOR

Potential, mv vs SCE

−1500 −1400 −1700 −900 −500 0 +200 +400 +800 +1000 +1400 +1800

was iodine reduction and the general anodic reaction was iodide oxidation. The small cathodic currents were due to depletion of iodine by the bubbling procedure.

More reproducible polarization curves were obtained in 1000 ppm KI-500 ppm I_2 solutions in which no attempt was made to remove oxygen. These solutions were merely covered by a helium atmosphere. As seen by curve B of Figure 3 cathodic portions of the potentiostatic polarization curves were less complicated than anodic ones. From an open circuit potential of 420 ± 20 mv vs. SCE, cathodic currents became diffusion controlled. The reactions most likely occurring were:

$$I_2 + 2e^- \rightleftharpoons 2I^- \text{ and/or}$$
$$I_3^- + 2e^- \rightleftharpoons 3I^-$$

The current was limited by the diffusion of I_2 and/or I_3^- to the 321 stainless steel surface.

A second "reduction wave" was observed near -400 mv. This wave may have resulted from the reduction of oxygen or of an oxygen-iodine complex. Currents increased sharply around -1000 mv due to hydrogen evolution.

The anodic curves were more complicated. There was no clear cut diffusion region. From open circuit, anodic currents increased immediately and rapidly reached larger values than those measured for the corresponding amount of cathodic polarization. The initial reaction most likely was the oxidation of I^- to I_2 and/or I_3^- and/or I_2 may then have been further oxided to $I(H_2O)_x^+$. Part of the anodic current could also have resulted from the slow dissolution of the steel. However, careful examination revealed no surface roughening.

Potentiostatic polarization curves were then measured
in solutions stirred by a magnetic stirring bar. As seen in
Figures 4 and 5 anodic curves for solutions containing 350 ppm
iodine were less sensitive to stirring than cathodic curves.
Upon stirring at a fixed rate, anodic currents increased by a
factor of two; cathodic currents increased by a factor of six.
No clearly defined anodic or cathodic diffusion plateaus were
found for stirred solutions. Due to the motion of the solution,
currents and potentials in stirred solutions were less stable
than in unstirred ones. In spite of this, the results indicate
that the reduction of iodine to I^- is largely diffusion con-
trolled because cathodic currents increased sharply upon stir-
ring. The oxidation processes may be controlled by both diffu-
sion and charge-transfer processes.

As shown in Figure 6, cathodic polarization curves
in unstirred I_2-KI solutions exhibited two well defined reduc-
tion waves. The first started at open circuit and had an
$E1/2 \sim +100$ mv vs. SCE,; the second started at -300 mv and had
$E1/2 \sim -540$ mv. It was conjured that the first wave was iodine
reduction to I^-, and that the second wave was either the reduc-
tion of an iron-iodine complex or a reduction reaction involving
oxygen. Attempts to deaerate I_2-KI solutions had not proven
helpful in idenifying the second reduction due to the rapid loss
of iodine. In order to overcome this difficulty, polarization
curves of 321 stainless steel were measured in solutions contain-
ing only KI.

As shown in Figure 6, the first reduction was absent
in both aerated and deaerated solutions containing 1000 ppm KI
and no iodine. In solutions containing iodine, the ratio of
limiting current to iodine concentrations (measured by thiosul-

Cathodic Polarization Curves

Fig. 4

350 ppm I_2, Stirring bar
350 ppm I_2, no stirring
210 ppm I_2, no stirring

Current
$\mu amp/cm^2$

Potential, mv vs SCE →

10
1000
100
10

0   −400   −800   −1200   −1600   −2000

Anodic polarization curves
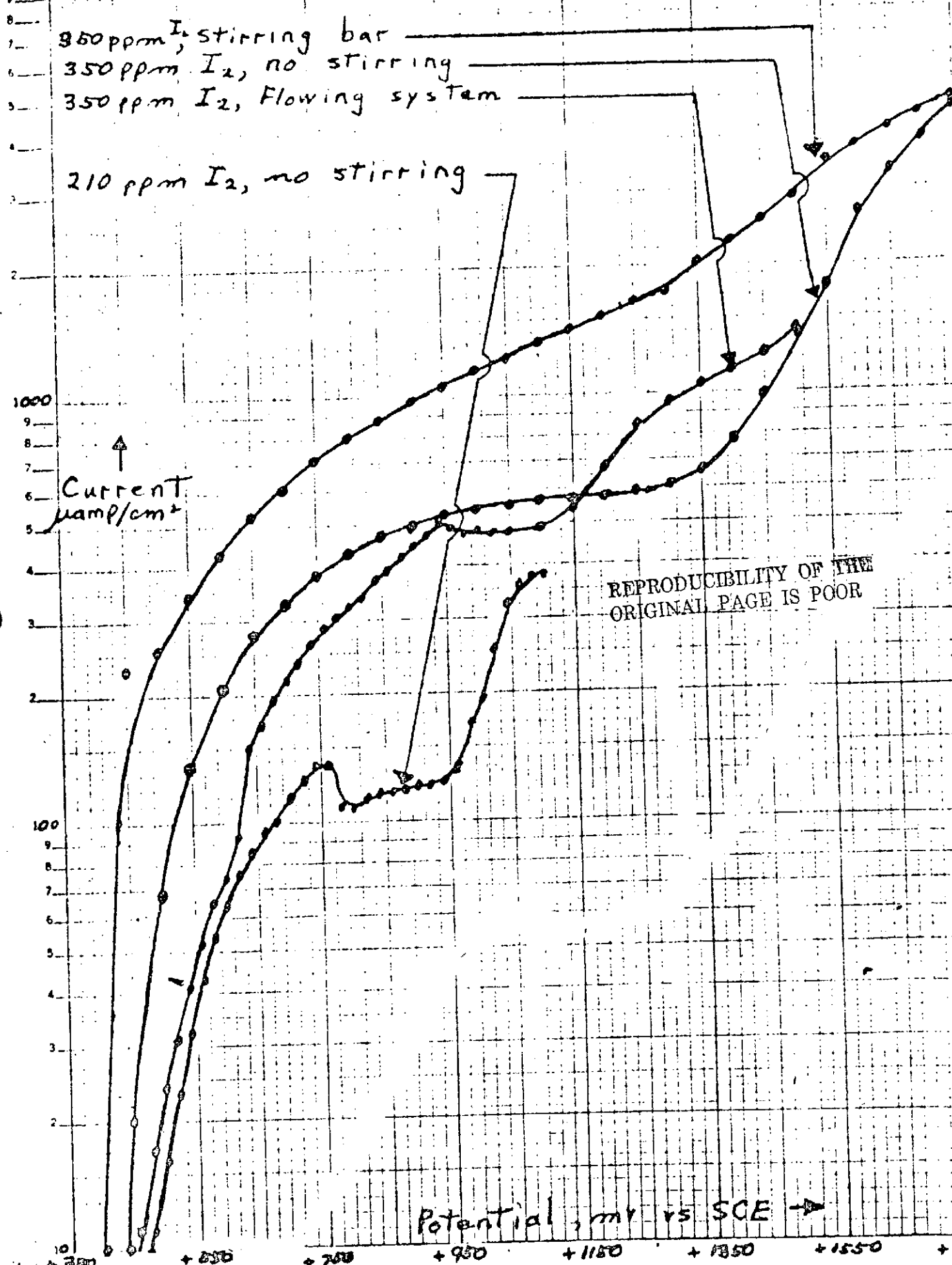
Fig. 5

350 ppm I₂, stirring bar

350 ppm I₂, no stirring

350 ppm I₂, Flowing system

210 ppm I₂, no stirring

Current μamp/cm²

Potential, mv vs SCE →

REPRODUCIBILITY OF THE
ORIGINAL PAGE IS POOR

Cathodic Polarization Curves   Fig. 6

220 ppm I_2 in a 1000 ppm KI solution, room conditions (O_2 present)
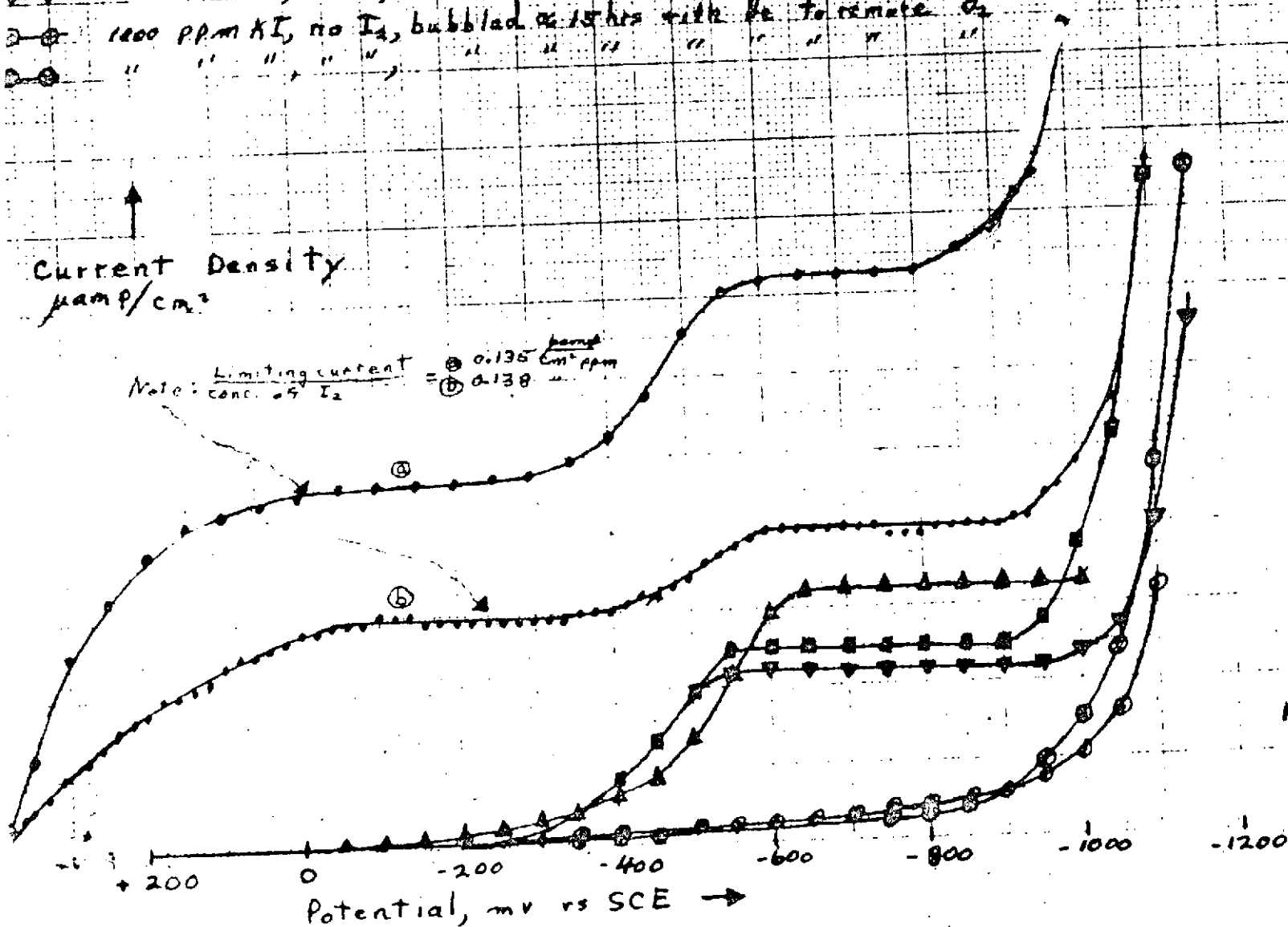210 ppm I_2 " " " " " " " "

1000 ppm KI, no I_2, room conditions (O_2 present)
" " " " , " " " " " " " "
" " " " , " " " " " "

1000 ppm KI, no I_2, bubbled ≈ 15 hrs with He to remove O_2
" " " " " , " " " " " " " " "

Current Density
$\mu amp/cm^2$

Note: $\dfrac{\text{Limiting current}}{\text{conc. of } I_2}$ = (a) 0.135 $\frac{\mu amp}{cm^2 \cdot ppm}$
                                                         = (b) 0.138 "

Potential, mv vs SCE →

+200   0   -200   -400   -600   -800   -1000   -1200

fate titration) was essentially constant at 0.14 µamp per cm^2 per ppm. These data indicate that the first reduction wave, indeed, is one or both of the following iodine reductions:

(1) $I_2 + 2e^- \rightarrow 2I^-$

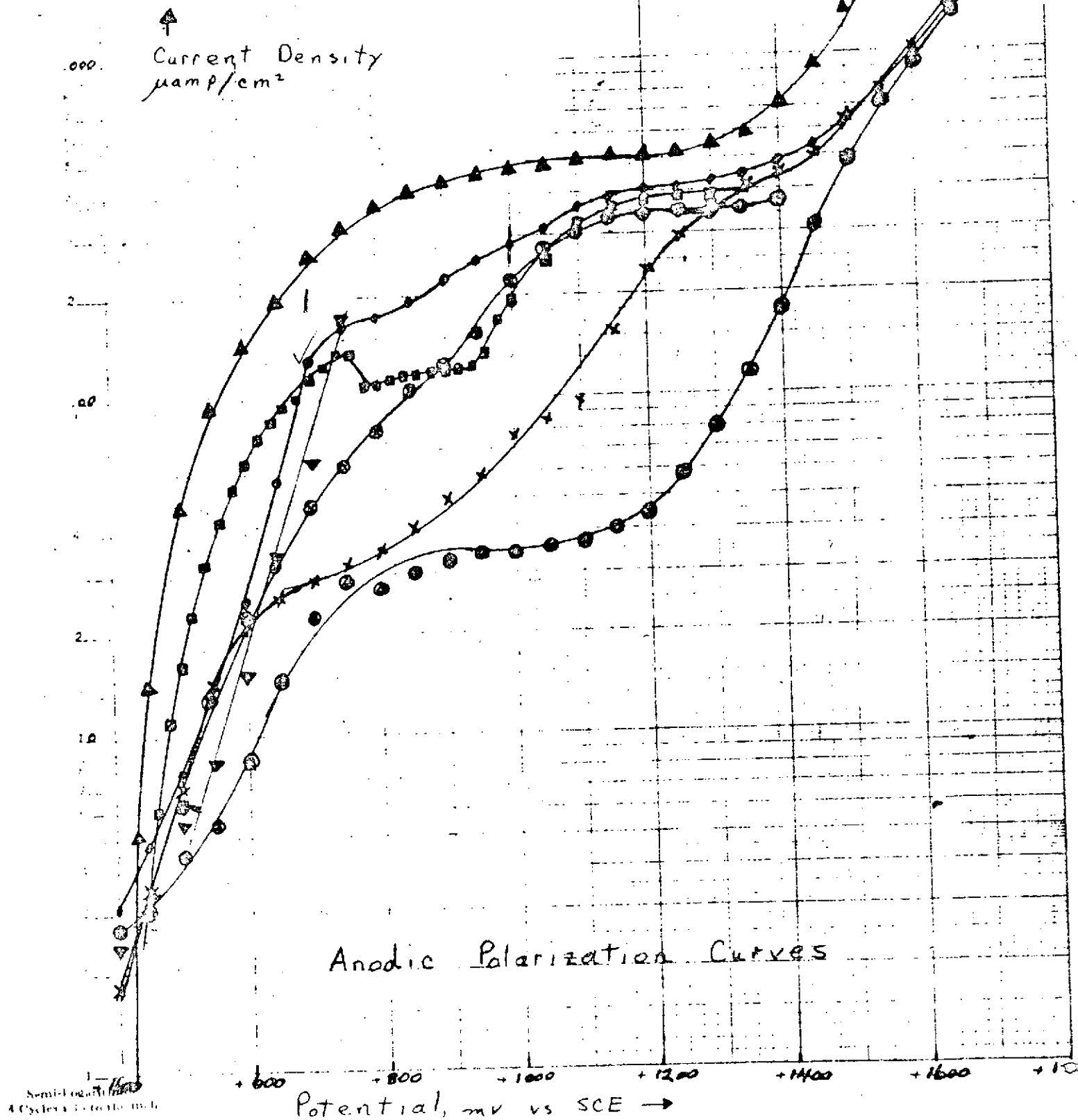(2) $I_3^- + 2e^- \rightarrow 3I^-$
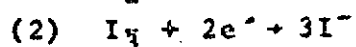
These reactions appear to be mainly diffusion controlled with some influence due to electrochemical control. Although the first reduction wave was absent in both aerated and deaerated KI solutions, the second wave was present in aerated solutions as also seen in Figure 6. The diffusion current for this wave in aerated KI solutions was approximately the same as the difference for the total diffusion current in I_2-KI solutions at the second wave, minus the diffusion current at the first wave. As also shown in Figure 6, both waves were absent in deaerated KI solutions. Cathodic polarization curves also were measured in deaerated KI solutions, which were then exposed to room air for twelve hours. In deaerated KI solutions, both waves were absent. In the air exposed solutions, the second wave again was present. These results indicate that the second reduction wave is due to a reaction involving oxygen.

Anodic polarization curves were also measured in aerated and deaerated KI solutions. Although in I_2-KI and KI solutions these curves are more difficult to reproduce than cathodic polarization curves, there were no dramatic differences in aerated and deaerated solutions, as shown in Figure 7. Also, there were no clear cut anodic diffusion regions.

As shown more clearly in Figure 8, open circuit potentials in KI solutions were about +50 mv vs. SCE, compared with +400 mv for I_2-KI solutions. Open circuit potentials also were less stable than in I_2-KI solutions. In KI solutions anodic currents remained small and relatively flat until an

▲ 350 ppm. I_2 in a 1000 ppm KI solution, room conditions (O_2 present)
● no I_2 present, 1000 ppm KI solution, room conditions, (O_2 present)
■ 210 ppm I_2 in a 1000 ppm KI solution, room conditions (O_2 present)
▼ no I_2, 1000 ppm KI solution, room conditions, (O_2 present)
✕ no I_2, 1000 ppm KI solution, room condition, (O_2 present). The cathodic polarization curve had just been run; the electrode had not been repolished.

⊗ no I_2, 1000 ppm KI solution, bubbled with Helium for 12 hrs to remove oxygen

⊕ no I_2, 111 ppm KI solution, room conditions (O_2 present)

↑ Current Density
$\mu amp/cm^2$

.000

2.

.00

2.

10

Anodic Polarization Curves

+600   +800   +1000   +1200   +1400   +1600   +1
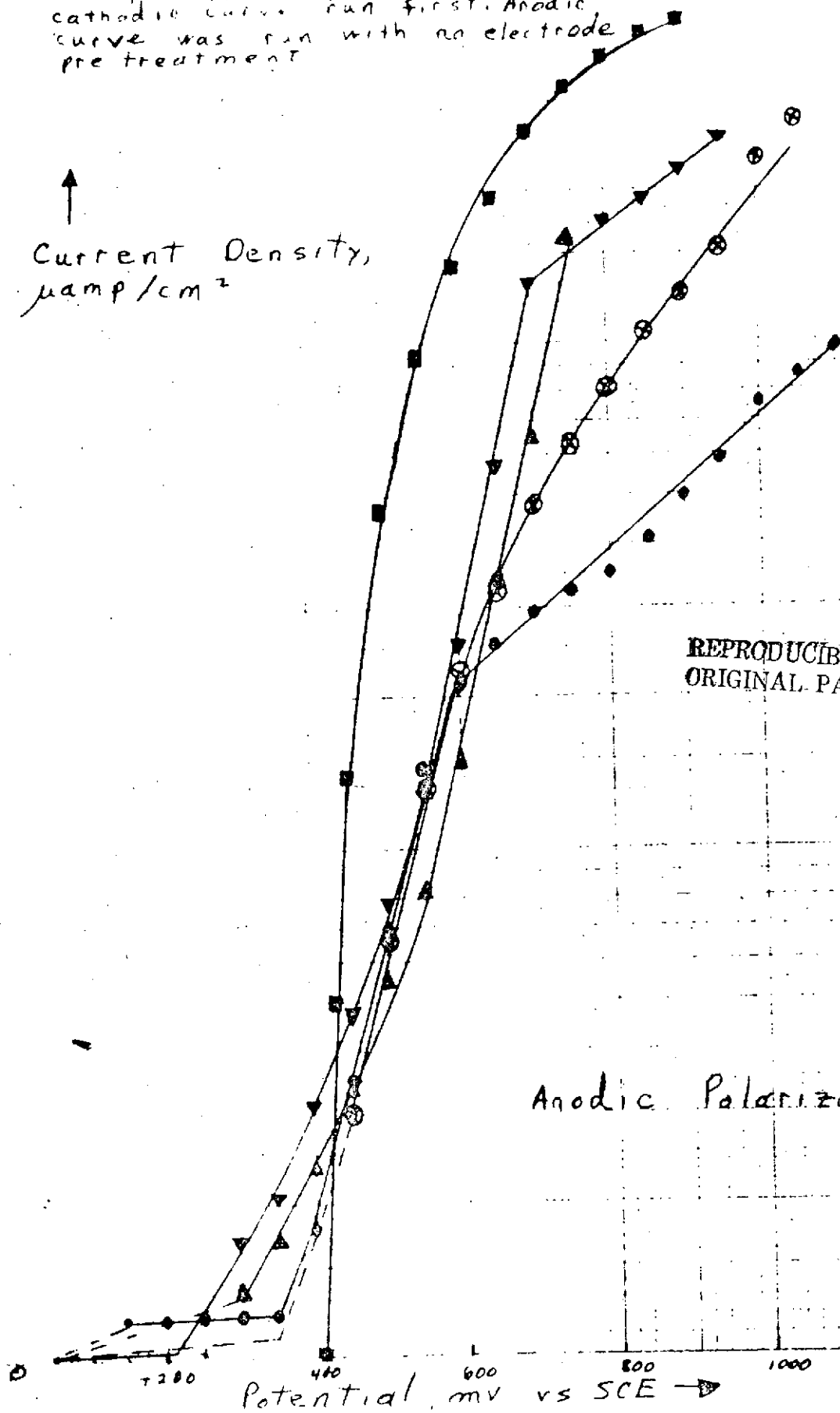
Potential, mv vs SCE →

Figure 8

■ 350 ppm I_2 in 1000 ppm hI solution, room conditions
▼ no I_2, 1000 ppm hI solution, room conditions
▲ no I_2, 1000 ppm hI solution, room conditions
⊗ no I_2, 1000 ppm hI solution, no oxygen
● no I_2, 1000 ppm KI, room conditions, cathodic curve run first. Anodic curve was run with no electrode pre treatment

Current Density, $\mu amp/cm^2$

Anodic Polarization Curves

+200   400   600   800   1000   1200
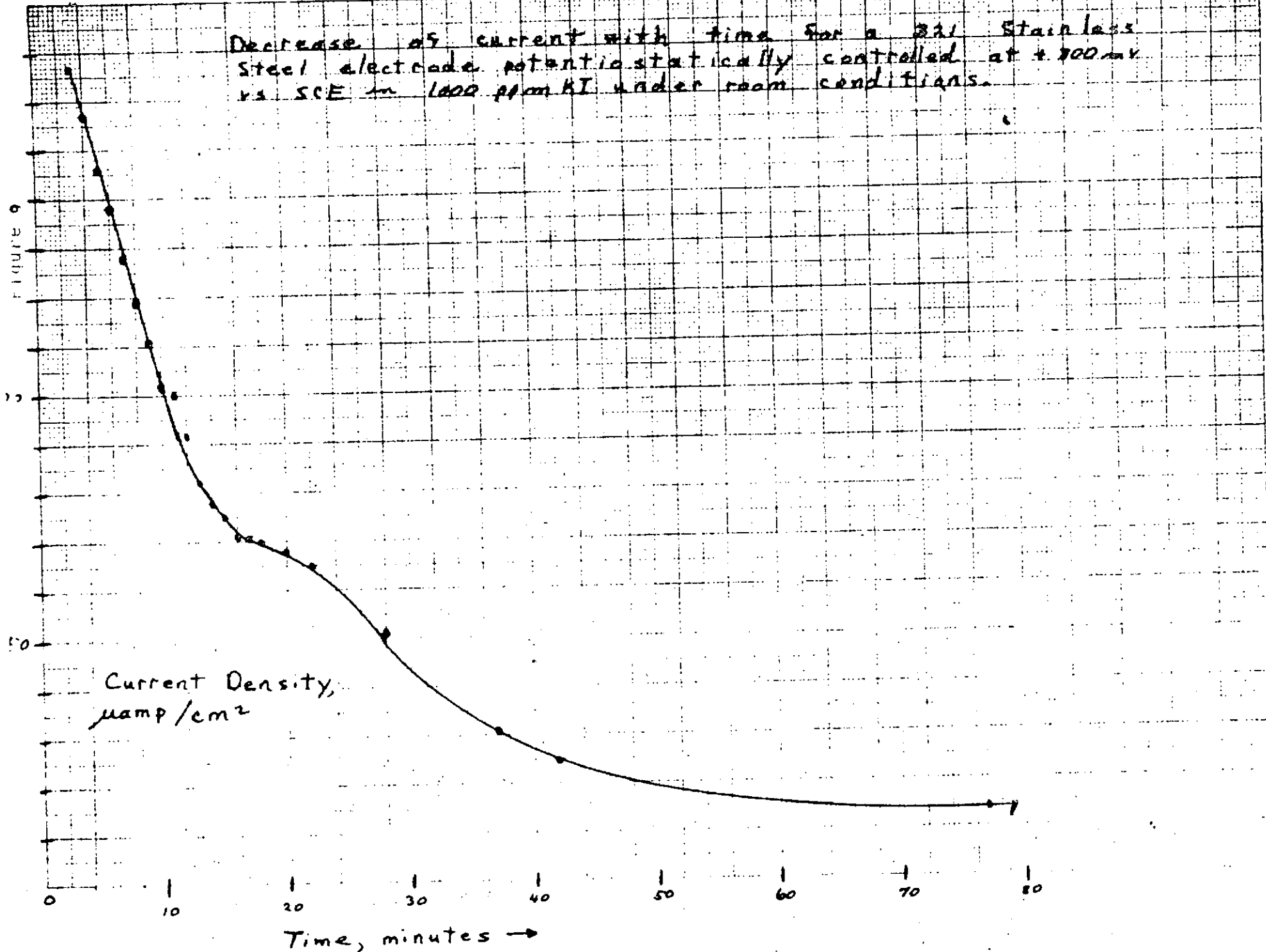
Potential, mv vs SCE →

0

Decrease of current with time for a 321 Stainless
Steel electrode potentiostatically controlled at +700 mV
vs SCE in 1000 ppm KI under room conditions.

Current Density,
μamp/cm²

Time, minutes →

oxidation "wave" started near +300 mv. Along this oxidation
curve, a faint reddish color due to iodine evolution could be
seen. In going from +400 mv to about +750 mv, anodic currents
increased with time, but near +750 mv began to decrease. This
decrease of current with time is illustrated in Figure 9 for a
321 stainless steel electrode maintained at a constant poten-
tial of + 800 mv in a 1000 ppm KI solution. Between +750 mv
and +1500 mv, currents decreased with time.

After an entire anodic polarization experiment (i.e.,
the electrode was polarized at each potential for two minutes
in steps of 50 mv up to +2000 mv vs. SCE), a dark film was
visible on the stainless steel surface. When the electrode
was held in flowing tap water for five minutes, the film did
not dissolve. However, when the electrode was placed in acidic
KI, the film quickly dissolved to give an iodine color to the
solution. When starch was added, the solution turned deep blue,
indicating the presence of iodine. Thus, the film is believed
to be precipitated iodine.

The potential at which the dark film developed was
then investigated. This was done by maintaining the stainless
steel electrode at selected anodic potentials for 45 minutes.
At +800 and +1000 mv, there was no clearly visible film. At
+1300 mv, a weakly attached film covered the surface. Near
the edges, the film was darker. Over the entire surface, very
small clear circles could be seen where possibly iodine or
oxygen bubbles had formed. At +1500 mv, the film was even dar-
ker and larger clear circles were visible.

In KI solutions, iodine evolution clearly occurred at
potentials more anodic than +450 mv. It is not clear if some

further oxidation to a $I(H_2O)+$ species occurred; however, the pale yellow color caused by iodine was not lost even after several hours at constant potentials more anodic than +800 mv.

As also shown in Figure 8, potential-log current plots between +400 mv and +750 mv were linear in KI solutions, but in the I_2-KI solutions they were not. From KI solutions, iodine evolution may then be controlled by a charge-transfer step. At a given potential in this range, currents for I_2-KI solutions (with approximately the same concentration of KI) were larger than for those in KI solutions alone. However, in both KI and I_2-KI solutions, anodic currents decreased or at least increased more slowly after +750 mv. This may be due to surface blockage by I_2.

III.

Iodine Production Rates

The next set of experiments consisted of measuring the rate of iodine production at selected potentials. The first attempt was to measure the iodine rate from a solution of approximately 12 ppm KI and 6 ppm I_2. In order to avoid large resistance drops in such dilute solutions, they were made 0.1 moles/liter in $NaClO_4$. As seen in Figures 10a, b, and c polarization curves of 12 ppm KI and 6 ppm iodine (the concentration of iodine was measured by the Beckman iodine meter) in 0.1M $NaClO_4$ were very similar in shape to previous polarization curves measured in solutions containing only 350 ppm iodine and 1000 ppm KI. Cathodically, there was again the reduction wave due to iodine reduction $(E_{1/2} \stackrel{\sim}{\sim} -200mv$ vs. SCE) and the second wave due to a reaction involving oxygen.

Anodically in 0.1M $NaClO_4$ the polarization curve was similar in shape to previous curves; however, a better defined oxidation plateau was measured.

Iodine production rates in this solution were then measured. As shown in Figure 11, iodine concentrations decreased with time at constant potentials of +750 and +850 mv vs. SCE. Iodine loss at open circuit was 0.88×10^{-2} ppm/minute (or about 0.5 ppm/hr) under room conditions. When the 321 stainless steel electrode was polarized anodically to +750 mv, the iodine loss increased to 2.23×10^{-2} ppm per minute. At +850 mv, the iodine loss was 1.92×10^{-2} ppm per minute. Environmentalmental conditions were the same in all cases. The data at +850 mv were taken after the solution was stirred for one

600m I_2 in 0.1 M $NaClO_4$

Current Density $\mu amp/cm^2$

Potential (ar vs SCE)

Cathodic Polarization Curves

Fig. 10b

● 350 ppm $I_2 + I_3^-$ in a 1000 ppm KI solution, room conditions

▲ 6 ppm I_2 + about 34 ppm $I^- + I_3^-$ in 0.1 M $NaClO_4$, "

Current Density $\mu amp/cm^2$

Potential, mv vs SCE →

Fig. 10c
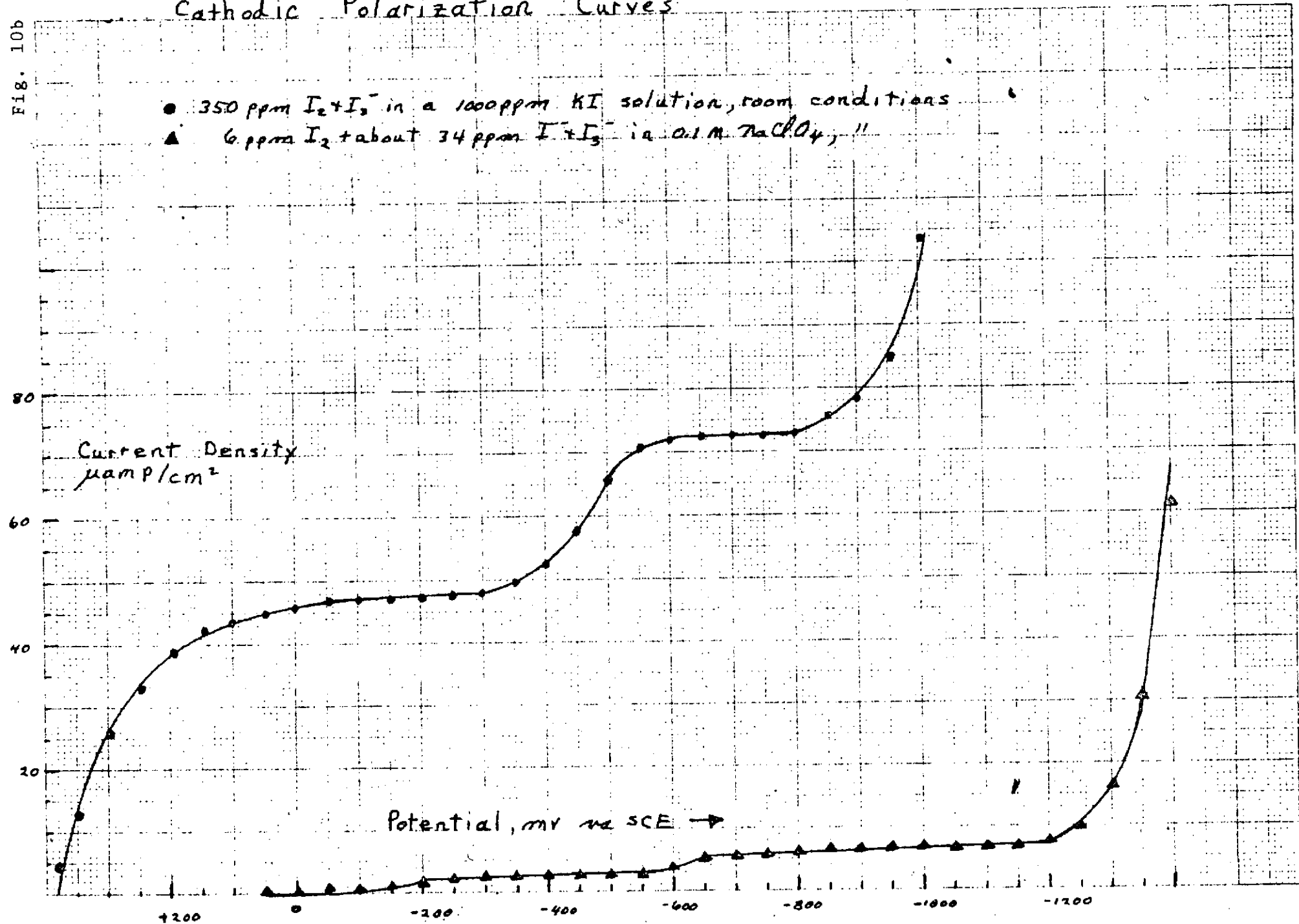
Anodic Polarization Curves

Supporting electrolyte was 0.1 M NaClO₄
321 Stainless Steel electrode.

⊗ 6ppm I₂, ≈ 20ppm KI + I₃⁻
● 10ppm KI, no O₂ present; rate of
   potential change was twice that of
   the other curves
▲ 10ppm KI, room conditions
■ 10ppm KI, room conditions
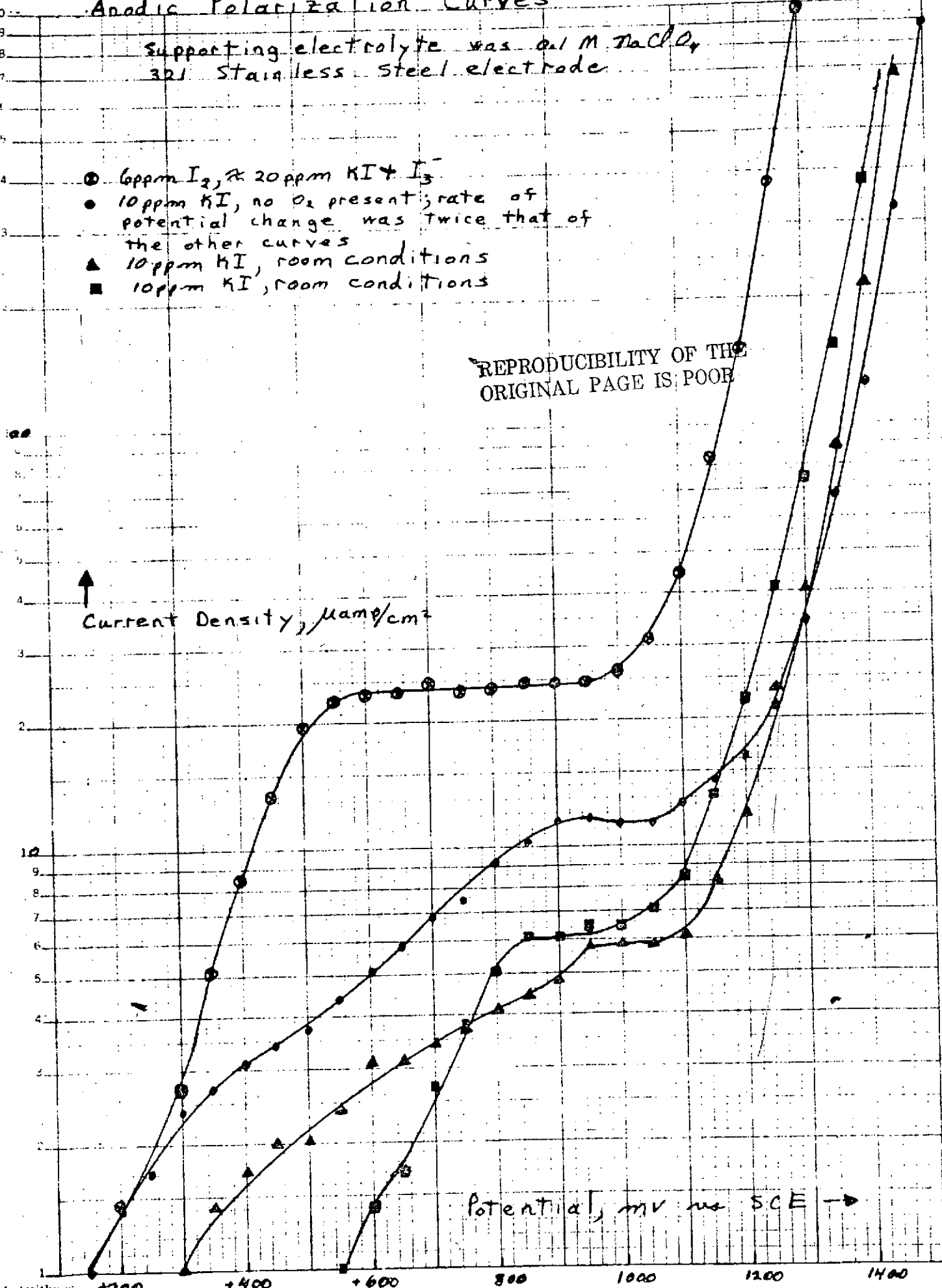
REPRODUCIBILITY OF THE
ORIGINAL PAGE IS POOR

Current Density, μamp/cm²

Potential, mv vs SCE →

+200   +400   +600   800   1000   1200   1400

Semi-Logarithmic
3 Cycles x 10 to the inch

Fig. 11
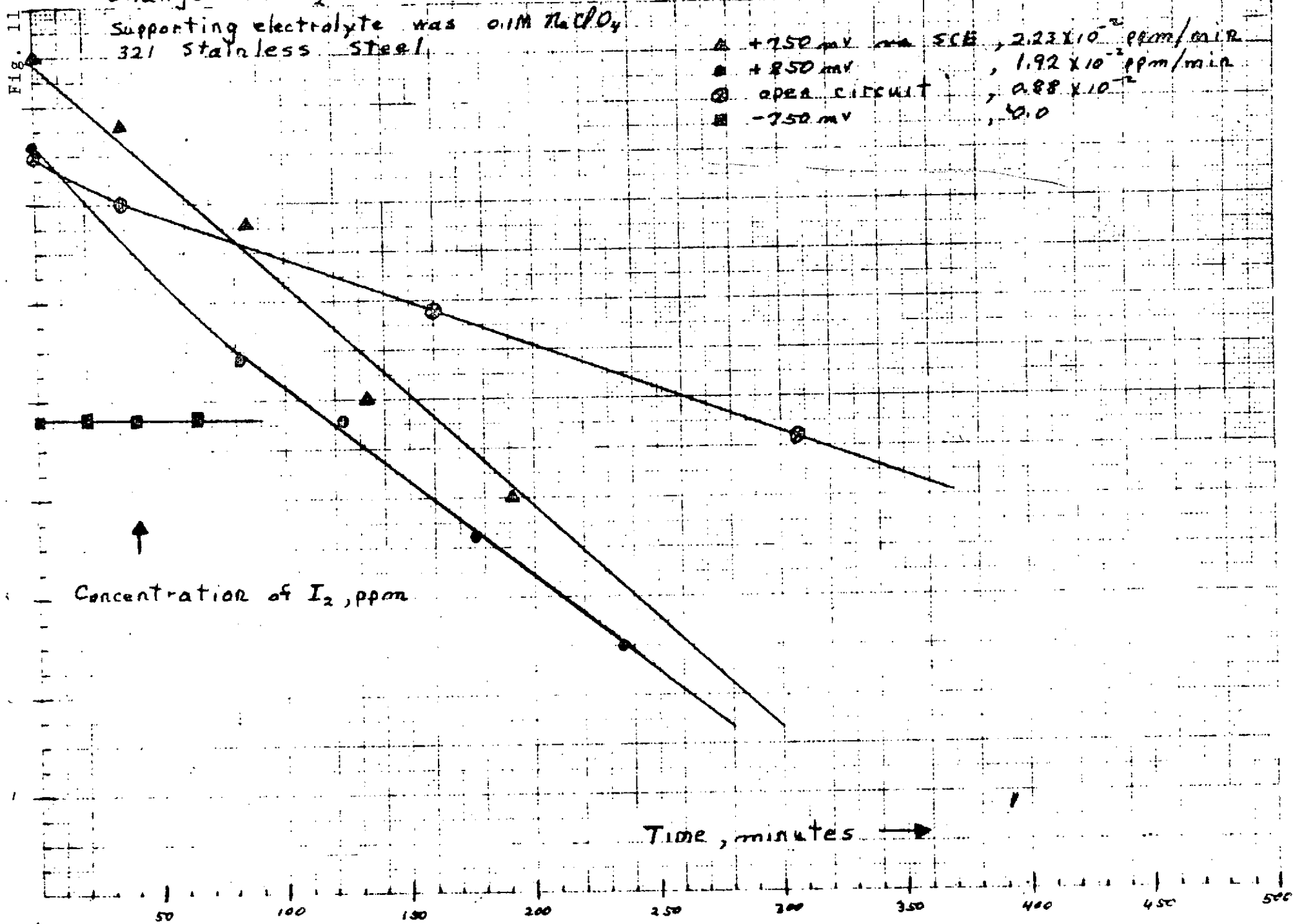
Change of I_2 concentration with time at constant potential. Supporting electrolyte was 0.1M $NaClO_4$. 321 stainless steel.

▲ +750 mv vs SCE , 2.23×10^{-2} ppm/min
● +850 mv , 1.92×10^{-2} ppm/min
⊗ open circuit , 0.88×10^{-2}
▣ -750 mv , 0.0

Concentration of I_2, ppm

Time, minutes →

50   100   150   200   250   300   350   400   450   500

minute before each iodine measurement. The better linearity
of the data indicates that briefly stirring the solution gave
a better distribution of iodine and more accurate measurements.

The loss of iodine upon anodic polarization in 0.1M
$NaClO_4$ indicated that some of the original iodine was oxidized
to iodate and/or some was reduced to iodide. Also the iodine
produced may not have diffused into solution and been measured
but was further oxidized to iodate.

Upon cathodic polarization the iodine concentration
remained almost constant. This may mean that the electrons
supplied at the stainless steel cathode were controlled by
the oxidation of iodide at the platinum anode. The two rates
were then equal.

The general loss of iodine in 0.1M $NaClO_4$ may also
have been due to experimental procedures. The concentration
was measured by placing the sampling tube of the Beckman iodine
meter directly into the reaction vessel. A piston in the meter
pulled or pushed the sample into or out of the instrument
sample chamber. After each datum point, the sample was re-
turned to the reaction vessel. Before each measurement, the
solution was stirree for one minute with a magnetic stirring
bar. This was done to distribute the iodine uniformly. These
procedures plus the volatile nature of iodine may have caused
the losses.

Because iodine was already present in the previous
solution, it could not be determined if it were even being
generated. In order to overcome this difficulty, the concen-
tration of iodine was measured as a function of time in solutions

of 0.1M $NaClO_4$ + 10 ppm KI. As shown in Figure 12, the iodine concentration remained essentially zero. These measurements close to zero iodine were less stable than those between 2 and 8 ppm. There appeared to have been a slight increase in iodine concentration between 100 and 350 minutes; after 350 minutes the iodine concentration again decreased. However, in this range, the values were within experimental error. At the end of the experiment a starch indicator was added; no blue color developed. Therefore, it is not believed that iodine was generated.

In order to insure that iodine was not being generated at the anode and then diffusing across to the platinum cathode and being reduced, the anode and cathode compartments were separated by a fritted disc. Again there was no measurable iodine production.

Previously, iodine had been visibly observed during anodic polarization of solutions 500 to 1000 ppm in KI alone. Iodine production was not successfully measured from).1M $NaClO_4$ containing up to 10 ppm KI. This lack of iodine production may have resulted from the oxidation of I^- directly to some $I(H_2O)_x^+$ species.

Efforts to produce iodine from solutions of 0.1M $NaClO_4$ + 10 ppm KI had been unsuccessful. These solutions were replaced by 500 ppm KI solutions. These 500 ppm KI solutions were chosedn to 1) eliminate complications due to $NaClO_4$, 2) provide higher conductivity than 10 ppm KI solutions, and 3) increase the I^- concentrations near the anode.

Iodine production rates from 500 ppm KI solutions were first measured in the single compartment cell shown in

Fig. 12

I₂ Concentration with Time

supporting electrolyte was 0.1 M $NaClO_4$ + 10 ppm KI
321 Stainless Steel electrode

⊙ +750 mv vs SCE , 0.0 ppm/min
▲ +1000mv " , 0.0 "
▣ +750 mv, separate , 0.0 "
anode + cathode compartments

Concentration of I_2, ppm

Time, minutes →

Figure 13. The concentrations of iodine as a function of time are shown in Figure 14 for this cell. In the unstirred solutions, iodine was clearly evolved from +650 mv vs. SCE to +750 mv. However, no definite relationship was evident between the potential and the amount of iodine produced. This may have been due to not placing the electrodes in the same position relative to each other for each experiment.

As seen in Figure 14, iodine concentrations in unstirred solutions increased until a limiting concentration was reached. The time to reach this limiting concentration varied from 110 minutes to about 300 minutes. From the rising portions of these curves, iodine production rates ware estimated as 0.007, 0.015, and 0.060 ppm I_2/minute.

In unstirred solutions the iodine color was much more pronounced near the anode. The color slowly spread through the cell as the iodine slowly diffused from the anode. (Before each measurement the solution was stirred for one minute in order to obtain a representative sample.) It is conjectured that the iodine concentration increased until some diffused to the cathode and was reduced to I^-. Steady state conditions were reached in time in which the rate of iodine production was equal its lose by reduction, absorption and to the atmosphere.

An attempt was made to generate iodine in the same cell while constantly stirring the solution with a magnetic stirring bar. As seen in Figure 14, no increase in iodine concentration could be measured. Stirring may simply have increased its rate of transport to the cathode whare it was reduced back to I^-.
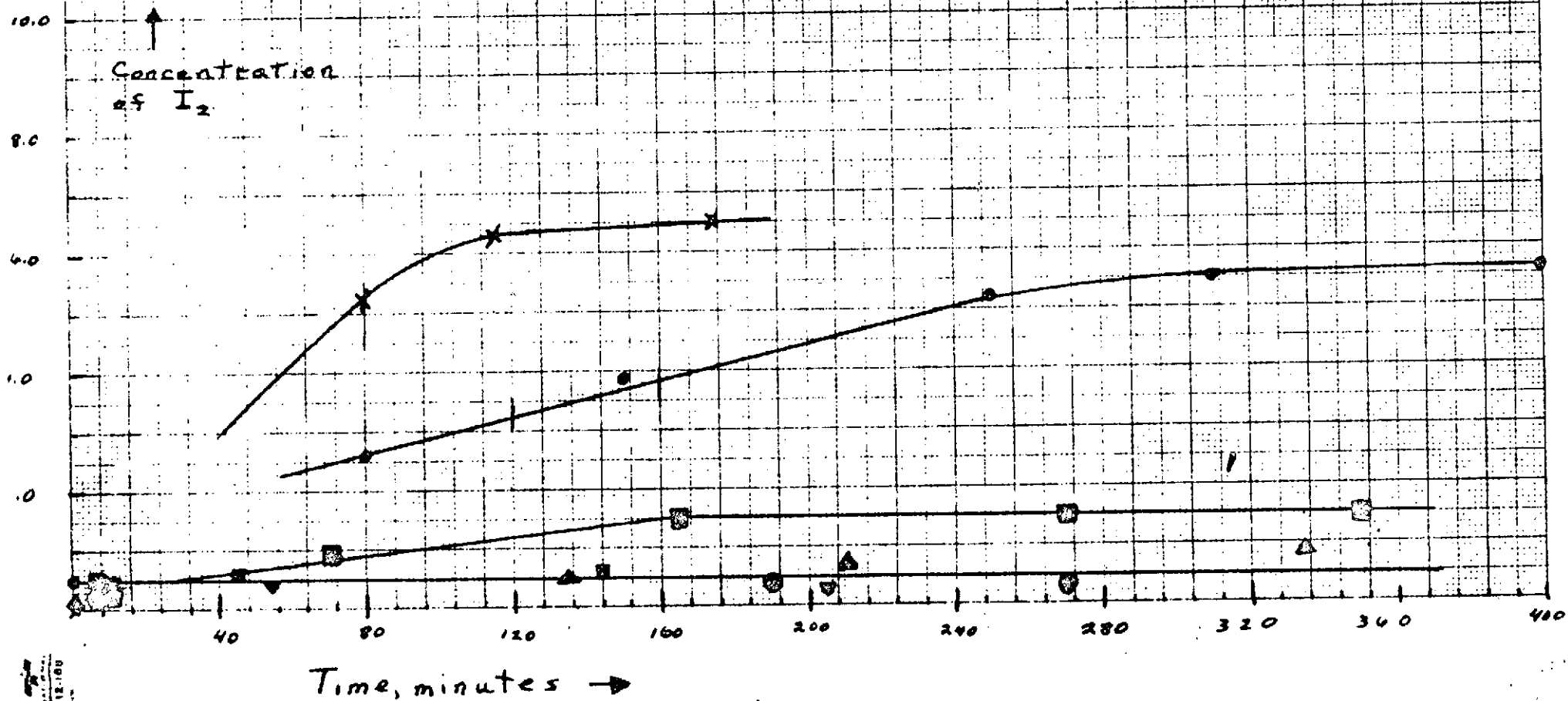
Fig. 13
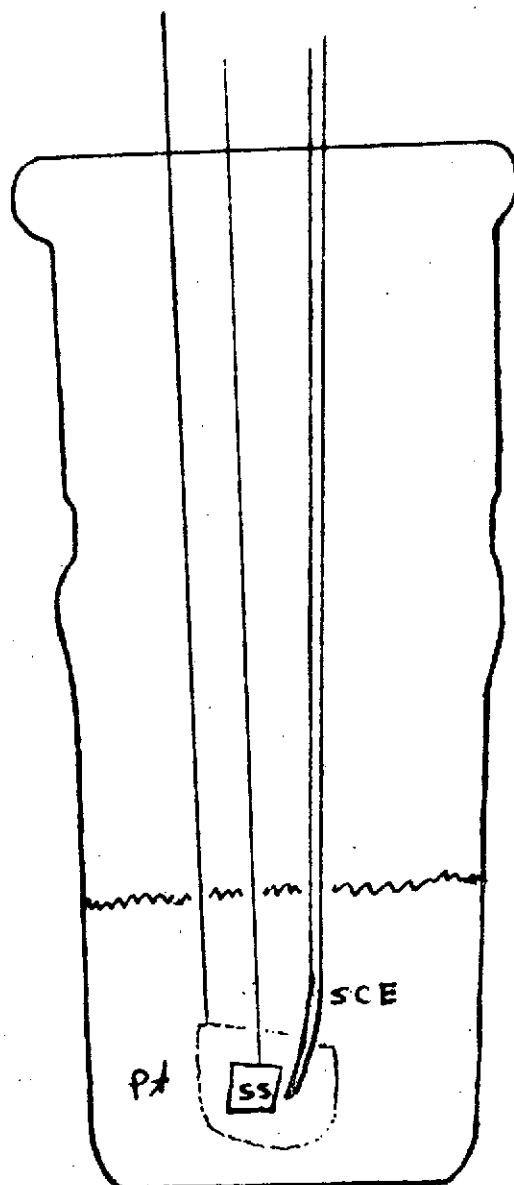
Single Compartment Cell,
Pt = Platinum Net, SS = 321 Stainless Steel,
SCE = Saturated Calomel Electrode

Fig. 14

Legend:
- ⊠ +650 mv, no stirring
- ● +750 mv, " "
- ⊞ +700 mv, " "
- □ +650 mv, stirring
- ▲ +500 mv, no stirring
- ▼ +750 mv, stirring
- ○ +750 mv, stirring

Rate of I_2 production from 500 ppm KI solutions. Room conditions. Anode and cathode were both in the same compartment.

Concentration of I_2

Time, minutes →

In order to eliminate the cathodic reduction of
iodine, the platinum electrode was placed in a compartment which
was separated by a fritted disc from the anode, as illustrated
in Figure 15. With this cell design iodine production rates
in unstirred 500 ppm KI solutions were approximately the same
as in the single compartment cell. However, over the time period
employed (maximum of 200 minutes) the iodine concentrations in-
creased linearly, as shown in Figure 16. When the solution in
the anode compartment was stirred, the iodine production rate
increased by a factor of about 5, which also can be seen in
Figure 16. In all cases when the cathode compartment was
analyzed, no iodine was detected; therefore, very little, if
any, iodine diffused through the frit.

In the two compartment cell, positioning of the stain-
less steel and the reference probe was very important for the
iodine production rate. Highest rates were obtained by placing
the reference probe in the middle and as close to the anode as
possible. When the reference probe was placed to the side and
more distant from the anode, iodine production, shown by the
bottom two curves in Figure 16, decreased even with stirring.

In each experiment the anodic current was measured.
In the two compartment cell the current increased with stirring
and appeared to be related to the iodine production rate. From
the plot of iodine production rates as a function of current in
Figure 17, it can indeed be seen that the anodic current is
linearly related to the iodine production rate. By using the
average anodic current, the weights of iodine expected in solu-
tion after 100 minutes (assuming all the current was due to the
$2I^- \rightarrow I_2 + 2e^-$ reaction) were calculated. In Figure 18, these
values are plotted versus the weight of iodine measured by the

Fig. 15
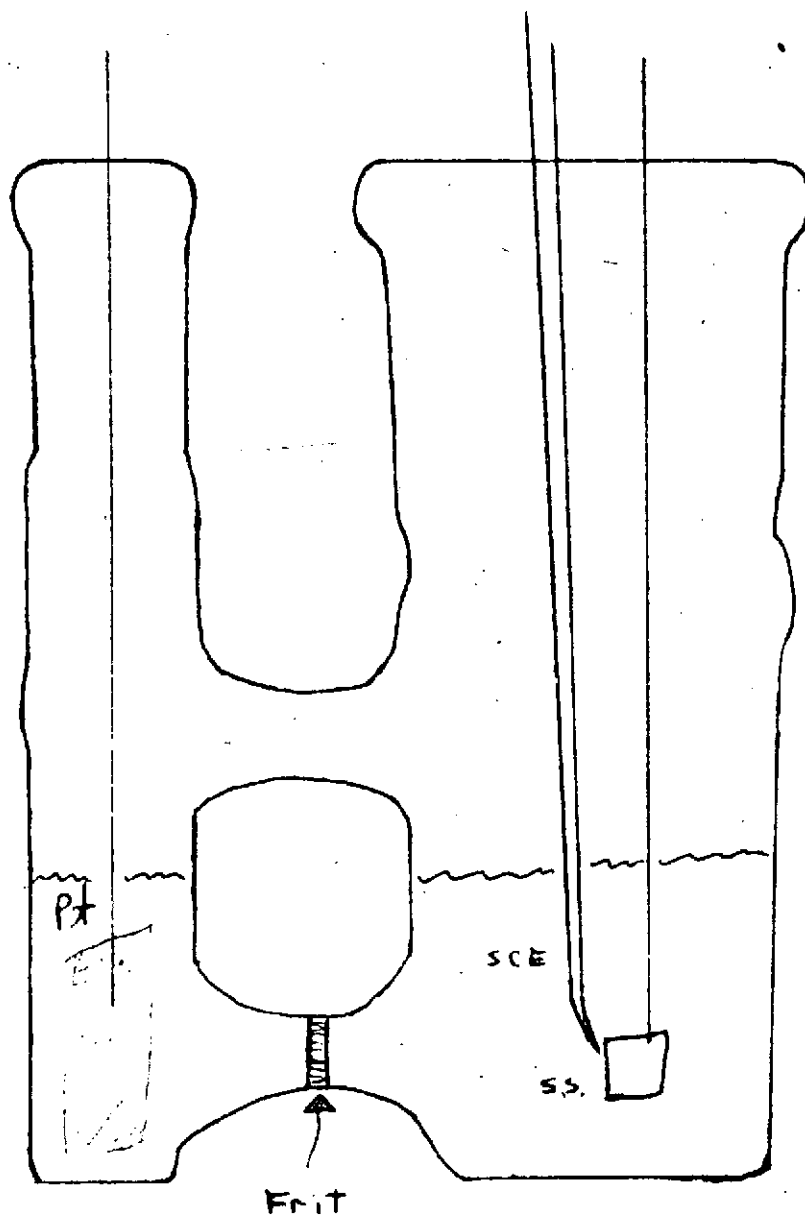
Two Compartment Cell, Pt= Platinum Aet, SCE= Saturated Calomel Electrode, SS= 321 stainless steel

Fig. 16

Rate of I_2 production from 500 mm KI solutions. Room conditions. Anode and cathode were in compartments separated by a glass frit.
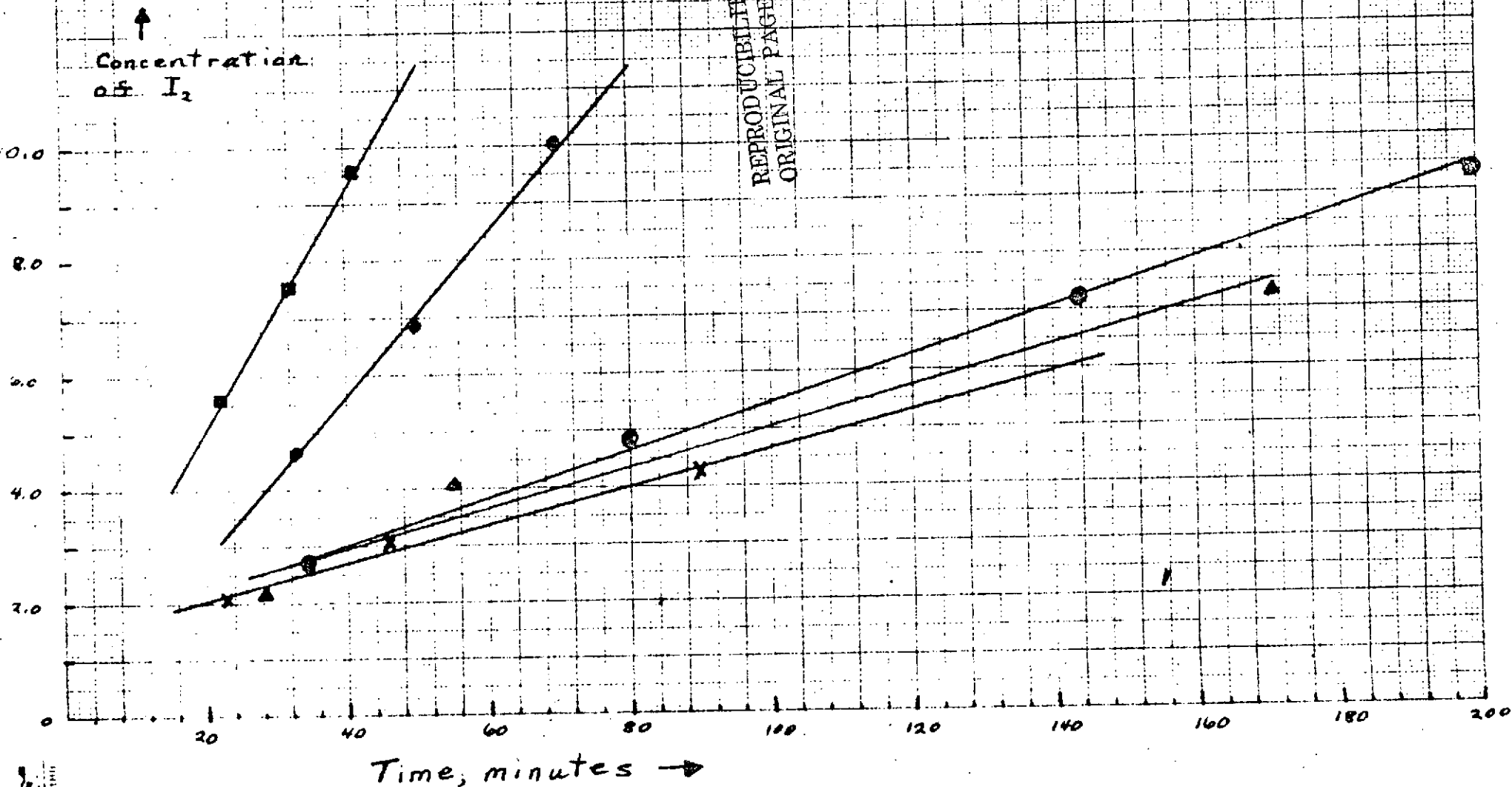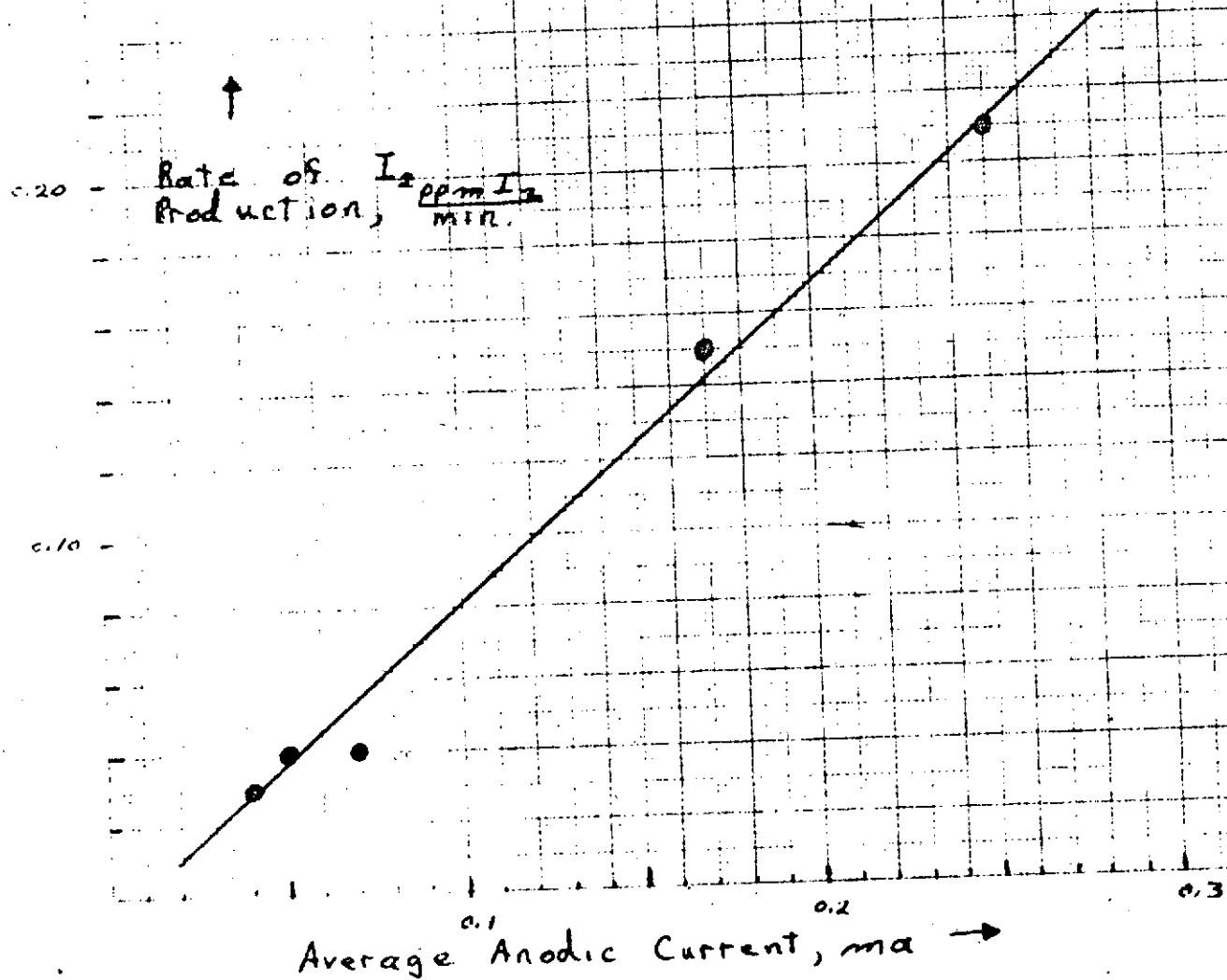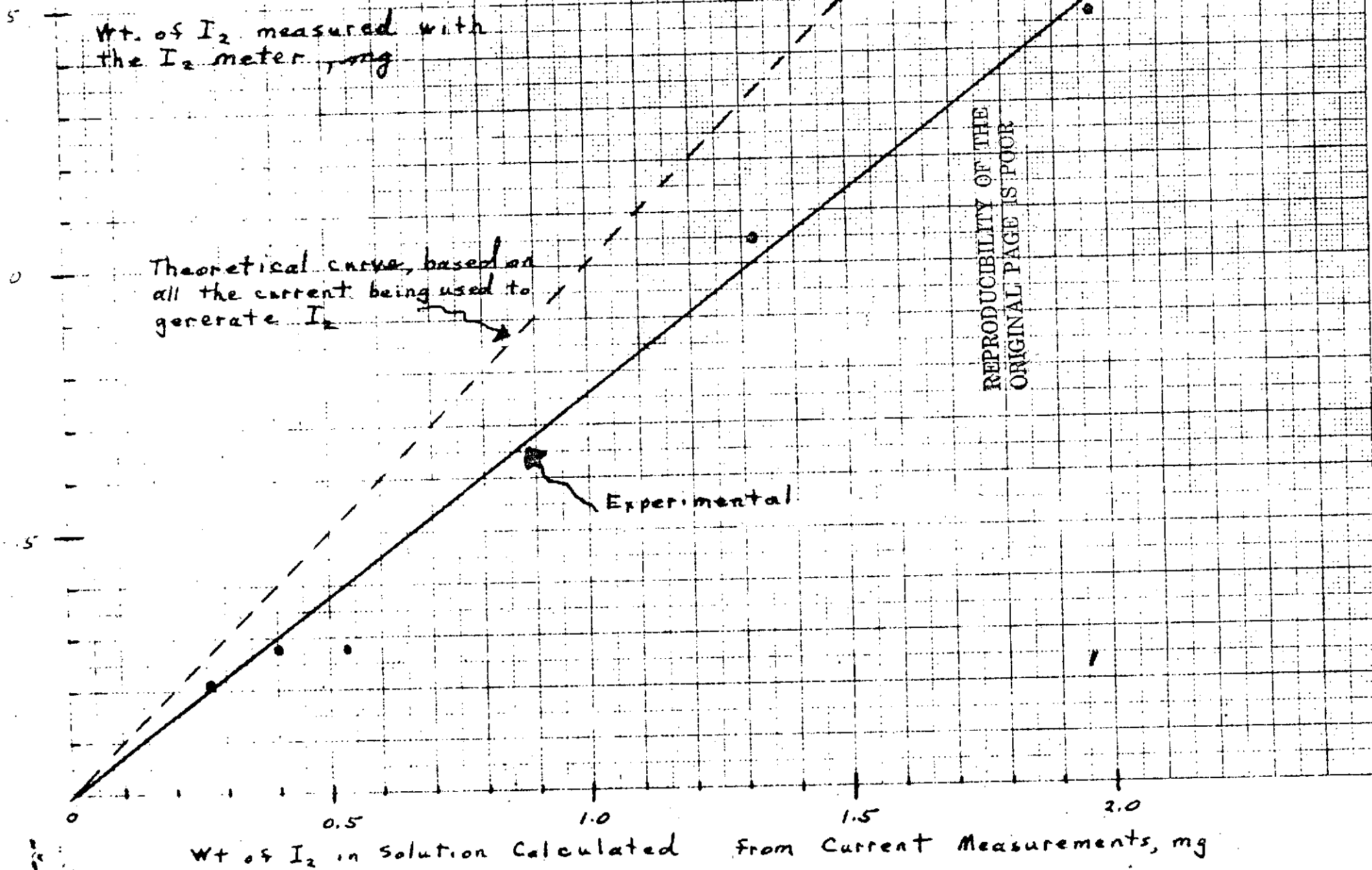
REPRODUCIBILITY OF THE
ORIGINAL PAGE IS POOR

Fig. 17

Relationship between rate of I_2 production and anodic current.

Rate of I_2 Production, $\frac{ppm\ I_2}{min.}$

0.20

0.10

Average Anodic Current, ma →

0.1   0.2   0.3

Fig. 18

Relationship between the measured I_2 in solution after 100 minutes and the weight expected (as calculated) from current measurements.

Wt. of I_2 measured with the I_2 meter, mg

Theoretical curve, based on all the current being used to generate I_2

REPRODUCIBILITY OF THE ORIGINAL PAGE IS POOR

Experimental

0.5   1.0   1.5   2.0

Wt of I_2 in Solution Calculated from Current Measurements, mg

Beckman iodine meter. This curve is then compared to the theoretical amounts expected. The amounts measured were 75% of the amounts expected from current measurements. Even if all the current were due to iodine production, some iodine would be lost due to absorption on the electrode and cell walls, absorption in the insulating material around the electrode, and simply to the atmosphere. Moreover, the high yield of iodine indicates that little of it is further oxidized to iodate.

The linear relationship between anodic currents and iodine production rates indicates that the anodic current can be used as an immediate gauge for achieving the best electrode design for maximum iodine production. That is, maximum iodine production rates should occur when the electrodes and potential are positioned and selected at maximum anodic currents.

Larger and more reproducible iodine production rates were obtained in the two compartment cell. However, by imposing a frit between the anode and cathode and by increasing the distance between these electrodes, the resistance between them also increases sharply. This larger resistance makes the potential and current more difficult to maintain and control.

In the two compartment cell iodine production rates were measured at a series of potentials from +600 mv to +1000 mv vs SCE.

Plots of iodine concentrations versus time shown in Figure 19 exhibit a tendency for the iodine concentrations to "level off" at longer time periods (greater than thirty minutes)

Fig. 19

Iodine production rates in 500ppm KI (382 ppm of I⁻)

Iodine rate
- +900 mv, 0.50 ppm/minute
- x +800 mv, 0.46
- ⊕ +1000 mv, 0.41
- ▼ +750 mv, 0.30
- ▲ +700 mv, 0.30
- ■ +600 mv, 0.23
- ◈ +850 mv, 0.36

Iodine concentration, ppm

REPRODUCIBILITY OF THE ORIGINAL PAGE IS POOR

Time, minutes →

and at larger iodine concentrations (greater than 10 ppm
iodine). The following explanation is offered to account
for this bending or leveling off. In all the experiments the
initial solution was 382 ppm in I^- (500 ppm in KI). The
largest iodine concentration measured was approximately 40
ppm, which is about 10% as large as the 382 ppm I^- originally
present. However, the iodine is believed to be formed mainly
by the reaction $3I^- \rightarrow I_3^- + 2e$. This means that for each iodine
ion measured, three I^- are consumed. For 40 ppm iodine, 120
ppm I^- would be consumed and only 262 ppm I^- would remain.
"Adjusted iodine concentrations" were calculated by multiplying
the measured iodine concentrations times the factor 382 ppm of
I^-/ppm of I^- remaining. These adjusted values then correspond
to the rates from a solution with a constant 382 ppm concentra-
tion of I^-.

As shown in Figure 20, iodine concentrations calcu-
lated in this manner increase linearly with time. The iodine
production rate at each potential is also listed in Figure 20.
In order to more clearly distinguish between lines, the +600,
+700, +750 and +1000 mv rates are plotted and listed in Figure
21. The +800, +850 and +900 mv rates are separately plotted
and listed in Figure 22. Because the data points in Figures
21 and 22 could be seen more accurately, the iodine production
rates listed in these figures are slightly different from the
rates in Figure 20.

In Figure 21 the iodine concentrations increase
linearly with time in an unbroken line. Although relatively
large errors are involved in measuring the external current,
it is interesting to note from Figure 23 that the currents
at these potentials change only slightly with time. Even

-16-

Fig. 20.

Iodine production rates based on a constant concentration of 382 ppm of I^- (assuming Iodine is formed by the reaction $3I^- \rightarrow I_3^- + 2e$)

Iodine rate

- ● +900 mv, 0.63 ppm/minute
- ✕ +800 mV, 0.63
- ⊛ +1000 mV, 0.49
- ▼ +750 mv, 0.39
- ▲ +700 mv, 0.37
- ■ +600 mv, 0.31
- ◆ +850 mV, 0.61
- ⊕ +850 mv, 0.58

Iodine concentration, ppm (assuming a constant concentration of I^-)
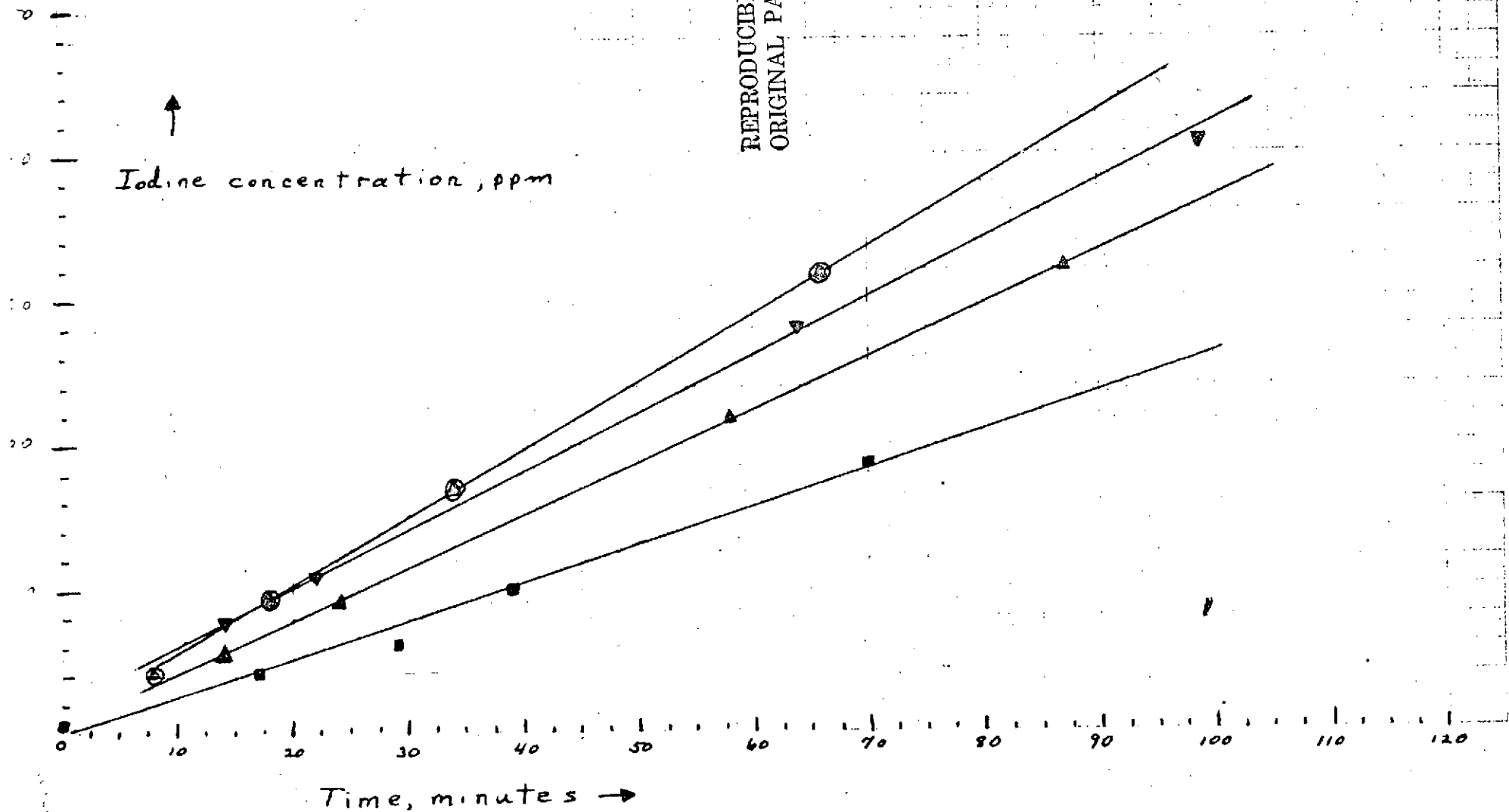
Time, minutes →

Fig. 21
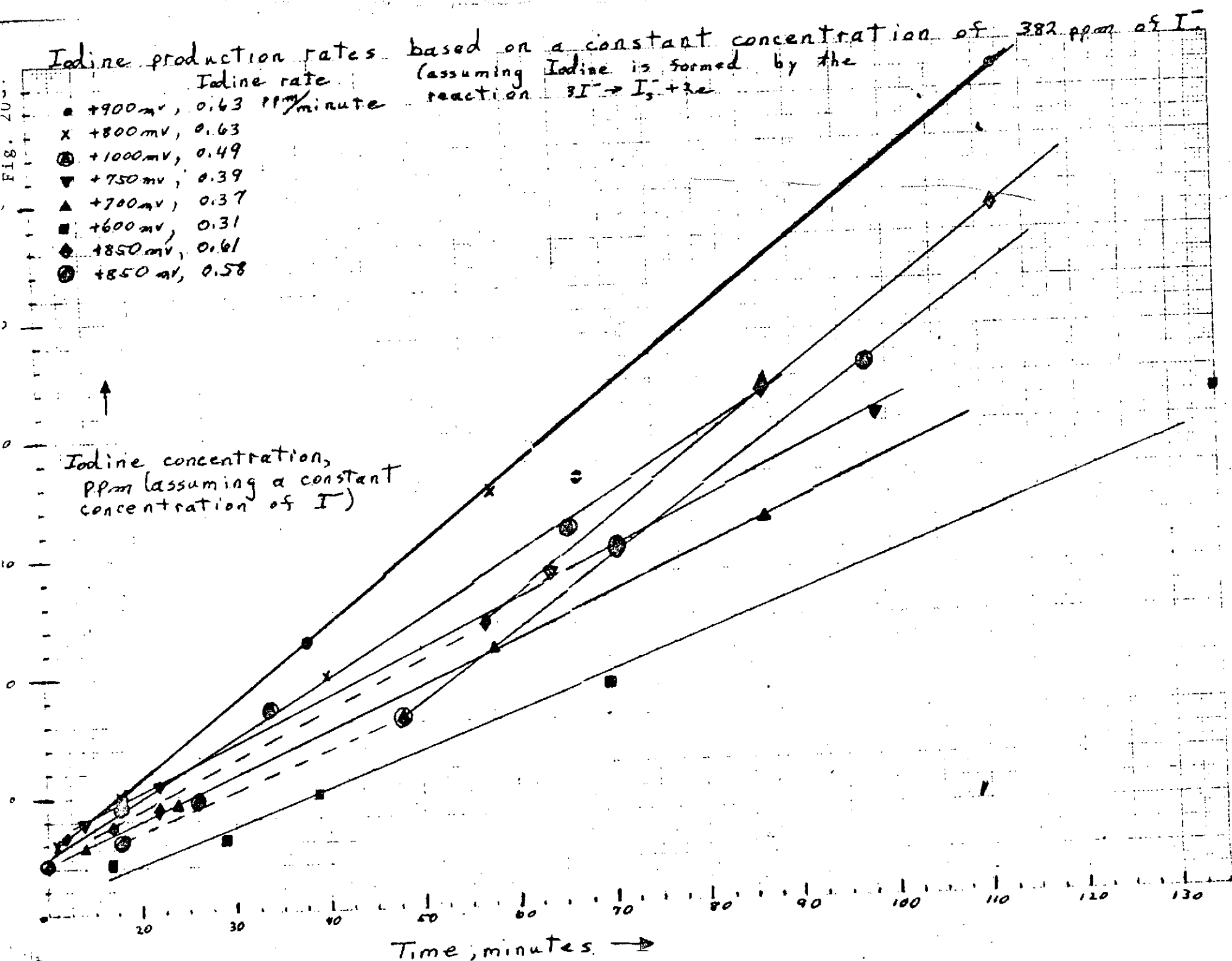
Iodine production rates based on a constant concentration of 382 ppm of I^-

- ⊕ +1000 mv, 0.46 ±0.01 11 m/min
- ▼ +750 mv, 0.40 ±0.01
- ▲ +700 mv, 0.36 ±0.01
- ■ +600 mv, 0.26 ±0.02

Iodine concentration, ppm

Time, minutes →

when the currents change, they change smoothly and with time reach a limiting value.

The +800, +850 and +900 mv rate data points in Figure 22 exhibit more scatter. In fact at +850 mv two slopes are evident, one of 0.39 ppm/minute and the second of 0.62 ppm/minute. Currents at these potentials were much less stable than those at the potentials listed in Figure 21. As seen in Figure 23 the currents generally increased with time and reached limiting values between 0.50 and 0.54 ma. For the +850 mv potential the larger slope (0.62 ppm/minute of iodine) corresponded to the higher currents. The true iodine production rate at +850 mv is believed to be this larger value.

The reason for this belief is as follows: to some extent, all the set potentials shifted to more cathodic values when the solutions were stirred. This was more evident at the +850 mv potential. With time the potentials shifted back to the set values, but at +850 mv this took longer (about fifty minutes). Potentiostats maintain a constant potential by changing the current. In the high resistance solutions used (500 ppm of KI in distilled water), the potentiostat, upon solution stirring, could not quickly sense the set potential. The currents and potentials were very unstable. Because of this no attempt was made to correlate the external current with the measured iodine production rates. Actual iodine production rates at a set potential were not obtained until the potential stabilized.

As shown in Figure 24, maximum iodine production rates were obtained at potentials from +600 mv to +900 mv vs. SCE. However, currents, potentials and iodine rates are somewhat less stable in this potential range compared to the range +600 mv to +800 mv.

Iodine production rates based on a constant concentration of 382 ppm I⁻

Fig. 22

●	+900 mv	0.62 ± 0.03 ppm/min
X	+800 mv	0.62 ± 0.03
◆	+850 mv	0.62 ± 0.01
◉	+850 mv (repeat)	0.55 ±

Iodine concentration, ppm

Time, minutes →

Fig. 23 — Change of current with time

Legend:
- X +800 mv
- ● +900 mv
- ◉ +850 mv
- ◆ +850 mv
- ⊕ +1000 mv
- ▼ +750 mv
- ▲ +700 mv
- ■ +600 mv
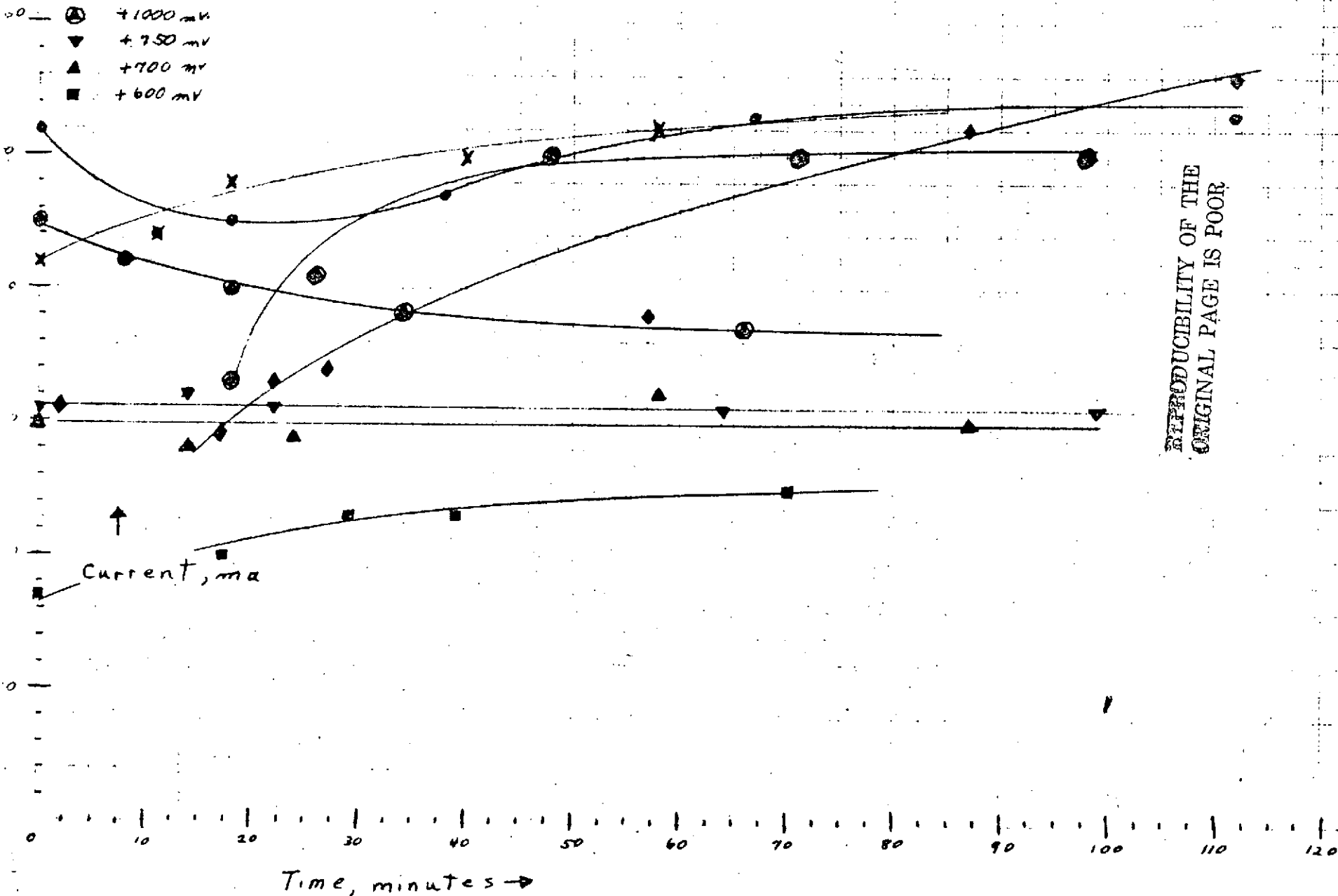
Current, ma

Time, minutes →

Fig. 24 — Relation between potential and Iodine production rates

Iodine production rate, ppm/min; a constant I^- concentration of 382 ppm was assumed.

Potential, mv vs SCE →